Air Flow separation above unsteady breaking waves

Nicolas Reul, Hubert Branger, Jean-Paul Giovanangeli

Air-flow separation over unsteady breaking waves

N. Reul, H. Branger & J.P. Giovanangeli

Institut de Recherche Sur les Phénomènes Hors Equilibre,
IOA, Campus de Luminy - Case 903,
13288 Marseilles Cedex 9, France
e-mail:nicolas@pollux.irphe.univ-mrs.fr

Abstract

Experiments were conducted in the small IRPHE wind-wave facility to determine the instantaneous response of the air flow over short unsteady breaking waves. Breaking was induced at a specific location in the tank by focusing wave energy of a single mechanically generated group under wind forcing. Instantaneous velocity and vorticity fields were measured over the highest and breaking wave of the group using the digital Particle Image Velocimetry technique. Measurements show that the air flow separates downwind of an unsteady breaking crest and then induces large perturbations in the air. The dynamics and geometrical properties of the separation bubble are strongly linked to the evolution of the wave. Locally, the momentum input from wind to water is strongly affected by this mechanism.

1 Introduction

Understanding the air-flow dynamics above short breaking waves (wavelengths of order 1 *cm* to 1 *m*) is of key importance for the parameterization of the momentum, mass and heat transfer between atmosphere and ocean. However, despite intensive theoretical and experimental investigation conducted over the last four decades, the structure of the turbulent flow over breaking waves is still largely unknown. It is now established that local air-flow separation occurs along with wave breaking (Banner & Melville (1976); Kawai (1982)) and that the separation process modifies the phase of the aerodynamic pressure relative to the surface wave (Banner (1990)). The separation mechanism modifies the local wind stress and may explain the discrepancy between observation and theory of growth rates (Belcher (1998)). At present, no realistic theoretical model of the flow over steep waves has been developed, and it is not known if the wind input to breaking waves with air-flow separation is large enough to be important in the balance of the short wave action equation.

In order to improve the modelling of the momentum fluxes from wind to water, direct observations of the air flow just above the water surface during unsteady breaking events are needed. In this paper we present experimental results on the evidence of air-flow separation and its effects on fluxes.

2 Experimental system and techniques

A series of experiments were performed in the small (8.0×0.6×0.6 m^3) IRPHE-Luminy wind-wave facility. The objective was to examine the evolution of the air-flow characteristics over the water surface during the passage of an isolated breaking wave propagating in a group. A schematic view of the experimental arrangement is shown in Fig 1. At the upwind end of the tank, a vertically oscillating wedge wavemaker produced a frequency-modulated wave-packet so that wave energy was focused at a predetermined time and location in the tank. The coalescence of this packet under a moderate wind forcing with a free-stream value of $U_o = 7\ m.s^{-1}$, led to the formation of a 0.4 s period breaking wave, at approximately 5 m from the tank entrance. To avoid perturbations in the air-flow, the wedge-wavemaker was completely immersed in the water at the end of the group generation. X-wire velocity measurements in the air at 5 m fetch ensured that there was no discernable wavemaker-induced wake at the time of passage of the breaking wave.

The instantaneous air-flow velocity field was obtained at the breaking region, using a cross-correlation Digital Particle Image Velocimetry (DPIV) technique. The flow was seeded with $8 \pm 5\ \mu m$ water droplets injected by a spray gun at the inlet of the flume. Two pulsed Nd:Yag lasers generated a light beam which was turned into a light sheet of about 1.5 mm thickness through a series of optics and mirrors. This light sheet was directed from above the tank towards the water surface and inclined at 10° from the vertical. It intersected the water surface creating a well-defined line, parallel to the wind direction and distant 15 cm from the tank side window. A PIV Dantec double-image CCD camera then recorded pairs of full-frame images of the illuminated particles above the

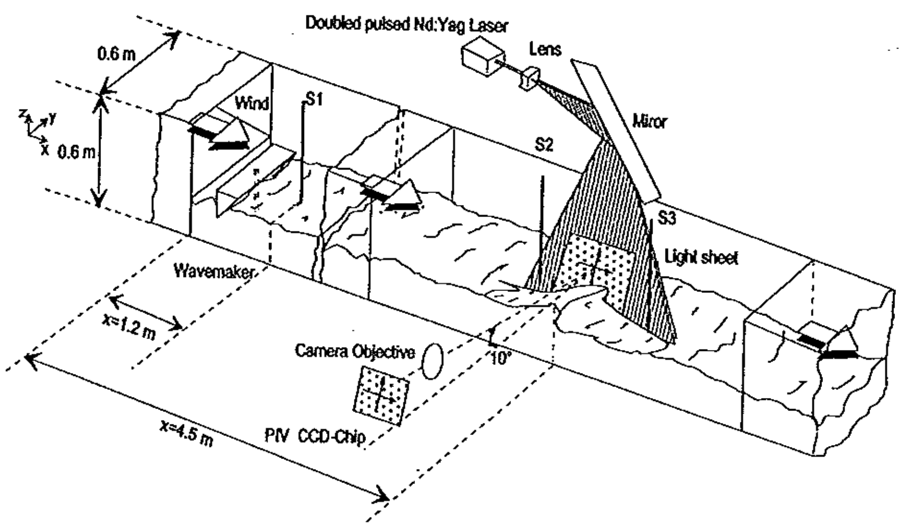

Figure1: Overview of the experimental arrangement

waves, viewing them from the side with an angle of +10° from the horizontal. The data acquisition process was synchronized with the signal sent to the wavemaker and triggered when the breaker crossed the camera field of view. The time separation between the two laser pulses was 100 μs and the actual field of view was 12.6×9.3 cm^2. This area was digitized at 768×484 $pixels^2$, and processed with interrogating cross-correlation window size of 32×32 $pixels^2$ with 50% window overlap. The data processing results in a field measurement of 47×29 velocity vectors and in a spatial wavelength resolution of 0.26×0.34 cm^2. DPIV images were first processed to detect the air-water interface and then were analyzed in the air free-surface region using the method of Dabiri & Gharib (1997) to obtain the velocity and vorticity field. An analysis of the overall error budget leads to an average relative error of 15 % for the velocity and 25 % for the vorticity values (Reul (1998)).

The fluid surface displacement was simultaneously measured in three different locations with three 0.3 mm diameter capacitance wire wave gauges. The breaker wavelength λ was obtained from the imaging of the water surface. The velocity of the breaking crest c_p was computed from two wave-gauge time series through nonlinear high-order analysis (Huang et al. (1998)). Static pressure fluctuations and velocity fluctuations were measured with a pressure probe and two hot wires in an X configuration located just above the surface.

3. General behavior of the separated flow

An example of the instantaneous air-flow velocity field over a spilling breaker measured in the laboratory frame of reference and the associated vorticity field is presented in Fig 2. Pictures were taken at the same location, and the time separation between two adjacent pictures is 135 ms. This figure shows clearly the occurrence of air-flow separation downwind of the breaking crest. First the flow was accelerated over the windward face of the crest, then a well organized roller-type motion with reverse flow appeared over the leeward face. The flow reattached on the windward face of the downstream wave. The flow does not separate over the first wave of the group. The separated flow is bounded from above by a high shear layer dominated by strongly localized coherent patches of vorticity. The shear layer departs from the interface at a point where the slope of the free surface exhibits an abrupt change. Small scale vortices appear in this initial region. They are convected in the shear region above the bubble of recirculation.

Different experimental conditions were conducted with various wind speed, wave amplitude, and wave steepness conditions. We have found that air-flow separation occurs over waves with local slopes greater than 35°. The area extension of the large scale vortex between the free-surface and the separated layer flow is an increasing function of the front-crest steepness ϵ_{crest}, defined as the ratio of the crest amplitude to the distance from the crest to the previous profile zero level crossing (Bonmarin (1989)). Figure 3 gives for $U_o = 7\ m.s^{-1}$ and for four typical front-crest steepnesses, the streamline patterns determined in a reference system moving with the phase velocity of the waves. Clearly the structure of the air-flow and more particularly the occurrence, the size and the extent of the air-flow recirculating bubble depend mainly on the local geometric properties of the wave. The center points of the separation bubbles appear as critical points of the flow associated with a convergence or divergence of the streamlines. It can be argued that near these points the air flow is largely three-dimensional with cross-wind components. From successive images, we have also determined that the vortex located in the center of the bubble moves downstream at the celerity of the wave. The life duration of the main vortex is linked to the duration of the breaking process. For very large values of ϵ_{crest} the flow does not reattach over the following wave: the separated area moves upwards inducing a large "bursting" process.

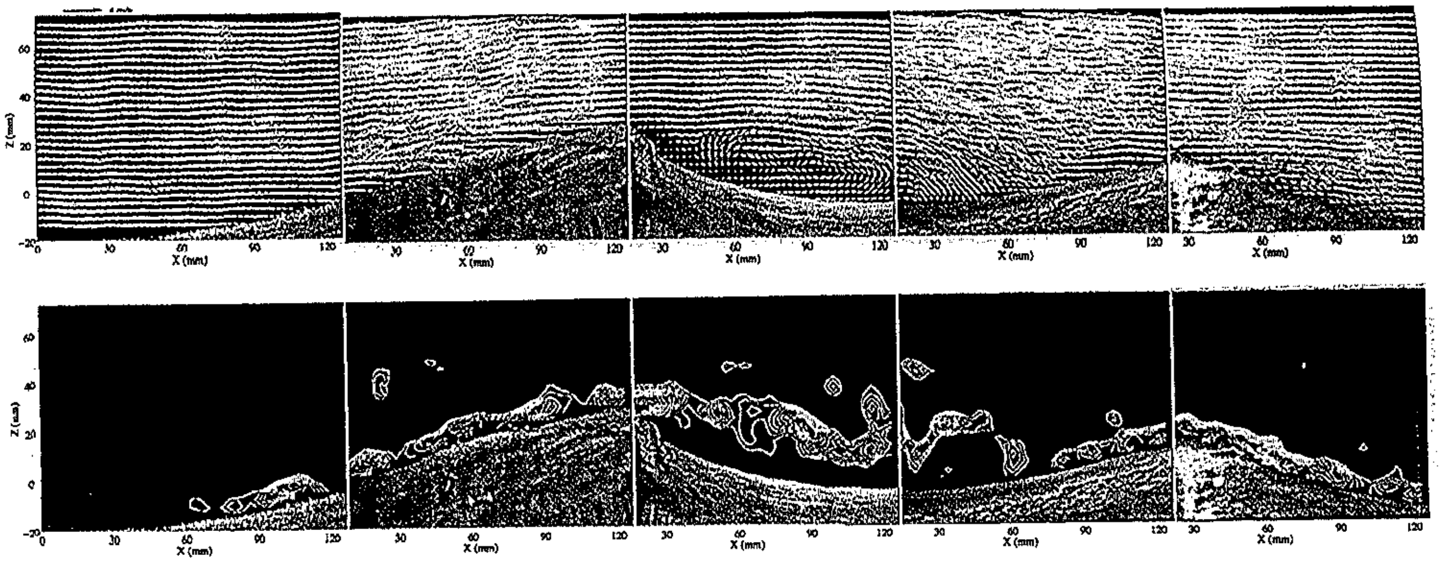

Figure 2: Air-flow instantaneous velocity distributions in the laboratory frame of reference (upper images) and corresponding contours of vorticity (lower images) over successively visualized sections of a transient spilling breaking wave. Minimum and incremental levels of vorticity are both $|\omega_{min}| = \Delta\omega = 100\ \mathrm{s}^{-1}$. Wind speed outside the boundary layer: $U_o = 7\ m.s^{-1}$. The time separation between two successive images is 135 ms

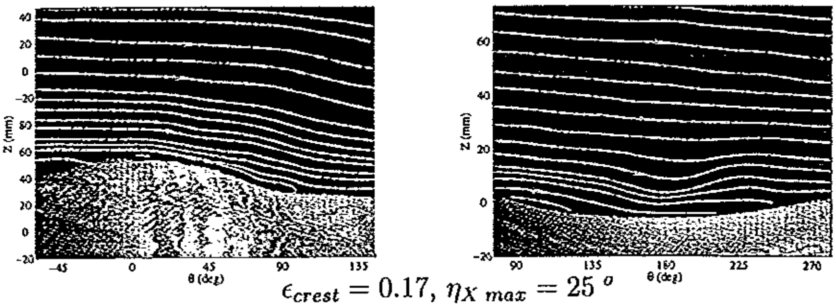

$\epsilon_{crest} = 0.17$, $\eta_{X\ max} = 25\ ^o$

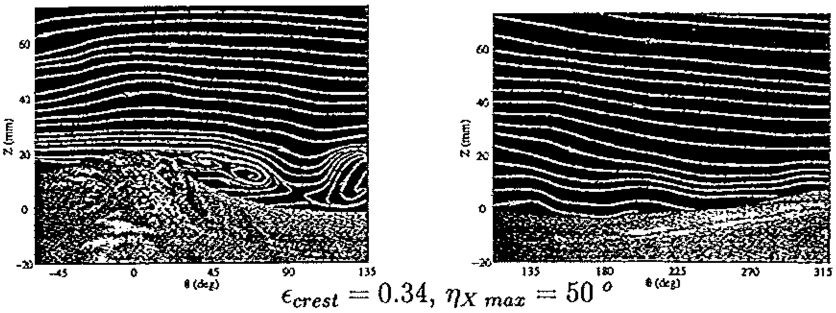

$\epsilon_{crest} = 0.34$, $\eta_{X\ max} = 50\ ^o$

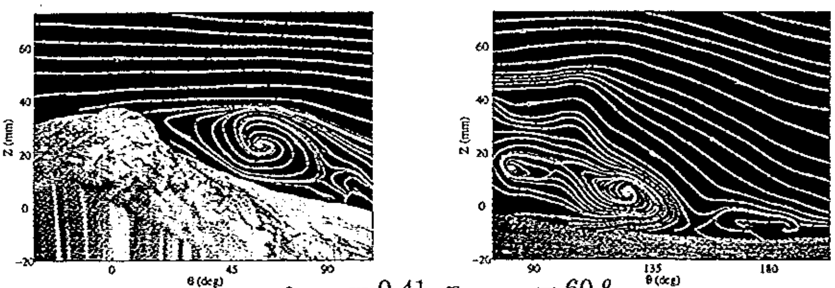

$\epsilon_{crest} = 0.41$, $\eta_{X\ max} = 60\ ^o$

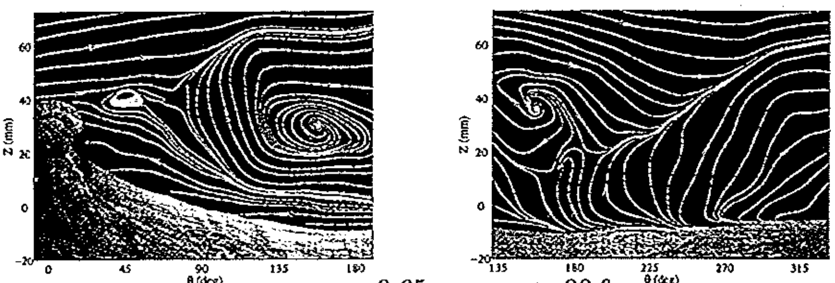

$\epsilon_{crest} = 0.65$, $\eta_{X\ max} > 90\ ^o$

Figure 3: Streamlines of the air-flow in the frame moving with the waves but for different front-wave steepnesses ϵ_{crest}. (θ is the phase of the wave; $U_o = 7\ m.s^{-1}$.). The time separation between the left and right images is 135 ms

4. Effects on momentum fluxes and conclusions

Previous studies have shown that breaking induces large spikes in momentum fluxe from wind to wave (Banner & Melville (1976); Banner (1990)) but no clear relationship has been given between the air-flow separation onset over unsteady waves and modification of the wind stress. By means of hot X-wires and a air static-pressure probe which have been operated in the close vicinity of the free surface, it was possible to connect the onset of air-flow separation with the modification of the turbulent boundary layer. Figure 4-a presents, for a case where air-flow separation occurs, time series of the water level measured by two adjacent wave gauges and the instantaneous product $-(uw)(t)$, where u and w are respectively the longitudinal and the vertical velocity in the air flow. It is shown clearly that the presence of steeper waves induces large enhancement of the product uw. That means that air-flow separation generated by the steep wave may infer a large contribution to the momentum flux $-\overline{uw}$. Figure 4-b presents, for the same experiment, the time series of the instantaneous pressure-slope product $(p\ \eta_X)(t)$. Here also, we observe large enhancements of this product which could induce a significant contribution to the the form drag $\overline{(p\ \eta_X)}$. We can then argue that the occurrence of the highest steep waves can induce a large burst in momentum transfer between air and waves leading to an increase of the form drag.

In conclusion, we have conducted PIV measurements of the air flow velocity and vorticity fields and pressure fluctuations above steep breaking waves generated in a small tank. The results show evidence of air flow separation above waves that exhibit high front-crest steepnesses. The separated flow is linked to the development of breaking. It serves as a strong intermittent source of turbulent vorticity in the air. Locally, the momentum input from the wind to the wave and the form drag are strongly affected. Breaking is a dissipation process but, by feedback, it can be a source of energy transfer from the air to the water. Statistical analysis of the whole set of PIV images are in progress to determine the geometrical and dynamical properties of the separated flow as functions of parameters related to both wind and waves.

Acknowledgment: This work has been supported by French Defense Department under Grant n^o94.34.147.00.470.75.01 and by French PATOM program.

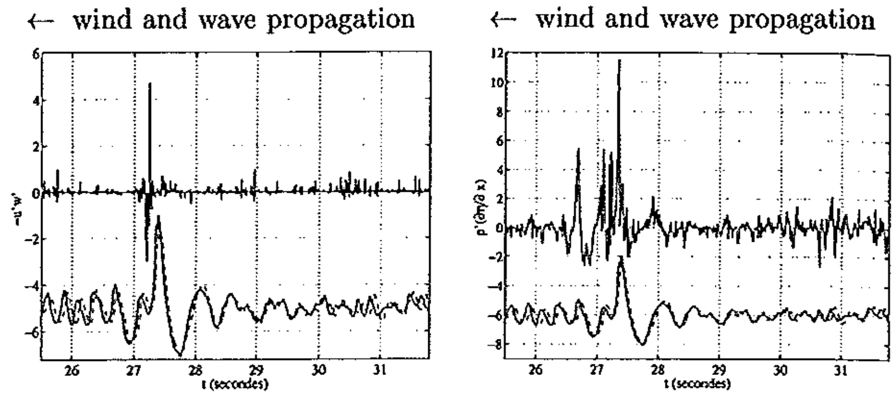

(a) (b)

Figure 4: Time series of water deflection level from two adjacent wave gauges and: a) instantaneous velocity fluctuation product $-(uw)(t)$ and b) instantaneous pressure-slope product $(p\ \eta_X)(t)$

References

Banner M.L., The influence of wave breaking on the surface pressure distribution in wind-wave interactions, *J. Fluid Mech.*, **211**, 463-495, 1990.

Banner M.L. & Melville W.K., On the separation of air-flow over water waves, *J. Fluid Mech.*, **77**, 825-842, 1976.

Belcher S.E., Turbulent flow over hills and waves, *An. Rev. Fluid Mech.*, **30**, 507-538, 1998.

Bonmarin P., Geometric properties of deep-water breaking waves, *J. Fluid Mech.*, **209**, 405-433, 1989.

Dabiri D. & Gharib M., Experimental investigation of the vorticity generation within a spilling water wave, *J. Fluid Mech.*, **330**, 113-139, 1997.

Huang N.E., Shen Z., Long S.R., Wu M.C., Shih H.H., Zheng Q., Yen N-C., Tung C. C., and Liu H.H., The empirical mode decomposition and the Hilbert spectrum for nonlinear and non-stationary time-series analysis, *Ph.. Trans. Roy. Soc. London* , 10, 903-993, 1998.

Kawai S., Structure of air-flow separation over wind wave crest, *Bound. Layer Met.*, **23**, 503-521, 1982

Reul N., Etude expérimentale de la structure de l'écoulement d'air au dessus de vagues courtes déferlantes, *Ph. D. Thesis*, Université de la Méditerrannée, IRPHE, 1998.

The Wind-Driven Air-Sea Interface

Electromagnetic and Acoustic Sensing, Wave Dynamics and Turbulent Fluxes

Edited by

Michael L. Banner

The University of New South Wales
Sydney, Australia

School of Mathematics
The University of New South Wales
Sydney, Australia

PROCEEDINGS OF THE SYMPOSIUM ON THE WIND-DRIVEN AIR-SEA INTERFACE

Electromagnetic and Acoustic Sensing, Wave Dynamics and Turbulent Fluxes

SYDNEY, AUSTRALIA
11-15 JANUARY 1999

ISBN 0 7334 0586 X

*PRINTED IN AUSTRALIA BY THE
ADFA DOCUMENT PRODUCTION CENTRE
CANBERRA, AUSTRALIA*